This study investigates the purification of ferronickel through electrolysis and precipitation processes to produce high-purity nickel. Ferronickel has yet to find extensive applications in industries requiring high-purity nickel. So, it is imperative to develop technologies that can upgrade ferronickel through electrolytic processes. Ferronickel, consisting of approximately 18% Ni and 80% Fe, represents an abundant but underutilized resource for high-grade nickel applications. Electrolysis was conducted using ferronickel anodes and graphite cathodes in 2 M HCl, followed by oxidation with H_2O_2 and precipitation with NaOH under varying pH (4.4 and 4.7) and temperature (40–70°C) conditions. Results demonstrated that the Ni concentration increased linearly from 5.36 g/L to 32.57 g/L over 8 hours of electrolysis, while Fe concentration rapidly increased and stabilized around 84.8 g/L after 3 hours. XRD analysis revealed improved crystallinity at higher temperatures, predominantly forming FeO_2 and NiO phases at 70°C. XRF analysis confirmed effective iron removal, achieving 78.91% Fe precipitation at pH 4.4 and 70°C, while nickel recovery was maximized at 14.60% at pH 4.7 and 70°C, but this pH is not favorable due to the Ni loss. SEM indicated finer, more homogeneous precipitate morphology at elevated temperatures. SEM imaging revealed that at pH 4.4 the precipitate formed at 40°C had a coarse, loosely packed structure with large, irregular particles (average size ≈ 6.50 μm). By contrast, at 70°C the precipitate was much finer and more homogeneous, with particles ~ 916.8 nm. The findings highlight that electrolysis follow by optimized precipitation enables efficient separation of nickel from iron, offering a promising alternative route for upgrading ferronickel without relying on HPAL or matte processes. This approach contributes to diversifying nickel supply chains and promoting sustainable raw material utilization using local content

Keywords: ferronickel, secondary, resources, local, content, electrolysis, precipitation, pH, temperature, time

UDC 669.24:546.74:541.124:546.26
DOI: 10.15587/1729-4061.2025.324608

ELECTROLYSIS AND PRECIPITATION-BASED PURIFICATION OF FERRONICKEL FOR HIGH-PURITY NICKEL PRODUCTION

Vita Astini
Student of Metallurgy and Materials Engineering*
Anne Zulfia Syahrial
Corresponding Author
Professor of Metallurgy and Materials Engineering*
E-mail: anne@metal.ui.ac.id
Johny Wahyuadi M.S
Professor of Metallurgy and Materials Engineering*
*Department of Metallurgy & Materials Engineering
Universitas Indonesia
Margonda Raya str., Depok, Indonesia, 16424

Received 10.03.2025
Received in revised form 16.04.2025
Accepted date 26.05.2025
Published date 17.06.2025

How to Cite: *Astini, V., Syahrial, A. Z., Wahyuadi, J. M. S., (2025). Electrolysis and precipitation-based purification of ferronickel for high-purity nickel production. Eastern-European Journal of Enterprise Technologies, 3 (6 (135)), 46–53. https://doi.org/10.15587/1729-4061.2025.324608*

1. Introduction

Nickel is one of the most essential mineral commodities for modern industry. According to the U.S. Geological Survey (USGS), global nickel production reached approximately 3.3 million metric tons in 2022 [1]. Of this total, Indonesia contributed an estimated 1.6 million metric tons, accounting for nearly 48% of global output, thereby solidifying its position as the world's largest nickel producer. Domestic electric vehicle production needs high supply of nickel as a raw material for batteries. One of the potential sources of nickel that can be used is to utilize local content Ferronickel (Feni) as secondary resource. Ferronickel is made by smelting high-grade nickel ore, producing approximately 18% nickel and 80% Fe. Nickel ore processing laterite as ferronickel is the most commonly used method in the industry today [2], so the ferronickel production is abundant. According to a report from the Directorate General of Metal, Machinery, Transportation Equipment, and Electronics (Ditjen ILMATE) of the Ministry of Industry, as of March 2024, there are 44 nickel smelters operating in Indonesia [3]. However, ferronickel has yet to find extensive applications in industries requiring high-purity nickel [4]. Consequently, ferronickel's production and market dynamics are predominantly influenced by the demand and supply fluctuations within the stainless-steel industry, where it is primarily consumed. So, it is imperative to develop technologies that can upgrade ferronickel through electrolytic processes.

Therefore, research devoted to the development of electrolysis-based purification and low-temperature precipitation techniques for ferronickel is highly relevant to support the transition toward sustainable nickel supply chains and the growing demand for battery-grade materials.

2. Literature review and problem statement

Several methods are considered to remove iron from nickel-rich solution. Electrolytic nickel (99.95% Ni) is produced from ferronickel by electrorefining using an anode with a nickel content of 80–85% [5]. However, there are limitations, including obtaining anode nickel with high purity, because Feni extracted from Ni laterite ore by the pyrometallurgical process has a Ni content ranging around ±20%. Therefore, not using an anode from available Feni but it created an anode material with a nickel composition exceeding 80%.

The paper [6] reported that the iron ion partly precipitated as magnetite by controlling the oxide potential and pH value. Magnetic separation offset the poor filterability of the precipitate. Iron (III) hydroxide precipitate formed during the coagulation to remove nickel ions from aqueous solutions [7]. But there is a problem with the loss of Ni during removal. The MHP precipitation method has been investigated for iron removal from nickel-pregnant leach solutions, ensuring that the precipitated nickel and cobalt remain free from iron compounds [8], but this research using synthetic pregnant leach solution that contain similar contain of Ni and Fe. Nickel powder was produced by electrodepositing nickel from boric acid, glycerol, and sulfuric acid [9], but this process is

very complex. The leaching of the battery cathode with HCl and H_2O_2 is used to recover Co metal with a process efficiency above 90% [10]. But requires high temperatures, as well as microwave and ultrasound, to speed up the leaching process. Moreover, while metal recovery is achieved, the purity of the recovered materials and their reusability in battery manufacturing are not explore yet. HCl has a higher activity coefficient compared to H_2SO_4. Although the two acids (1 M HCl vs. 1 M H_2SO_4) contain a different amount of H^+ ions in their structure, a likely explanation for faster dissolutions in HCl is the higher activity coefficient of chloride solutions when compared with corresponding sulphate solutions [11]. Previous research [12] investigation, higher molarity levels were associated with increased current, which resulted in faster reaction rates and increased nickel metal solubilization. However, the effect of time on the dissolution rate of Fe and Ni is not yet known, thus further research is needed

The problem statement of this research is how to purify Ni from ferronickel. Electrolysis process used to produce an electrolyte rich in Ni and Fe in ambience temperature. Because leaching process usually require higher temperature and also additional treatment to faster the process. Ferronickel is usually used in the stainless-steel industry, so if it is necessary to reduce the contamination of other elements, it will become a potential new source for battery materials. The first significant technical challenge in this research is how to control the electrolysis process of ferronickel to dissolve the Ni and Fe, and the second is how to precipitate Ni and Fe and separate them from the impurities.

3. The aim and objectives of the study

The aim of this study is to determine the effectiveness of electrolysis and precipitation processes for separate Ni and Fe from impurities and producing electrolytic Ni.

To achieve this aim, the following objectives are accomplished:

– to observe the effect of electrolysis time on Ni and Fe dissolved in electrolyte;

– to evaluate the pH effect on phases that form during the precipitation process;

– to analyze the effect of precipitation pH and temperature on the composition of the precipitate;

– to analyze the morphology and crystal size of precipitate that form during the precipitation process.

4. Materials and methods

This study focuses on the purification of ferronickel, a secondary nickel source, using electrolysis followed by selective precipitation to obtain high-purity nickel suitable for battery applications. The main hypothesis of this research is that ferronickel, despite its low initial nickel content (~18%) and high iron content (~80%), can be efficiently purified through electrolysis and moderate pH precipitation, enabling selective recovery of nickel while minimizing iron contamination. The experimental approach assumes that ferronickel can serve directly as an anode material without the need for complex pretreatment, and that operating under controlled pH (4.4–4.7) and temperature (40–70°C) is sufficient to achieve selective precipitation.

The anode for the electrolysis process is melted Ferronickel molded into 11 × 1 × 0.5 cm pieces (Fig. 1). The cast Ferronickel samples were separated according to predetermined measurements. Before the electrolysis procedure, the materials were cleaned with a grinding machine, and the weight was measured.

a *b*

Fig. 1. The local content sample: *a* — ferronickel shot; *b* — ferronickel blocks

An electric current passes through electrodes, and the charge moves between conductive media. Electrodes can be made of non-metallic conductors such as graphite but are more routinely made of metals such as zinc, copper, silver, or tin [13]. Graphite served as the cathode in the experiment, and the anode was a bar of ferronickel with the composition in Table 1. The graphite cathode is made of an 11-cm-long cylinder with a diameter of 1 cm.

Table 1

Composition of ferronickel shot

Element	Composition (wt.%)
Fe	77.369
C	1.140
Ni	18.490
Co	0.340
Mn	0.040
Cr	0.890
Si	0.430
P	0.017
S	1.275
Cu	0.009

The electrolyte solution, which was made using distilled water, was diluted in 37% hydrochloric acid (HCl). Hydrochloric acid is a strong electrolyte with widespread industrial use. Electrolysis times observe from one to eight hours were particularly examined for the 2 M HCl solution to identify the effect of electrolysis time.

The Electrolysis process produces a filtrate of metal ions like Ni^{2+}, Fe^{2+}, Co^{2+}, and other elements. The precipitation starts with the oxidation of the filtrate solution by hydrogen peroxide (H_2O_2). The oxidation process is essential in oxidizing Fe^{2+} ions to Fe^{3+}. The filtrate is precipitated by adding NaOH, increasing the pH to about 4.4 and 4.7. Filtration is then carried out to remove the filtrate from Fe residue to increase Ni concentration.

Atomic absorption spectrometers (AAS) are highly sensitive methods for analyzing elements, which is identification of metals in various samples at the picogram level. This ab-

sorption spectroscopy method uses the absorption of light by free atoms in a gaseous state to determine the quantitative composition of chemical components [14]. It is also used to determine the concentration of metals present in the analyzed sample. In this study, atomic absorption spectrometers were used to analyze the filtrate of electrolysis results to determine the composition of Ni and Fe metals in the sample.

X-ray diffraction (XRD) is analytical technique used in various industrial fields to study the physical properties of materials. This method is used to analyze the physical properties of the sample, such as phase formation/compound, crystal structure, and crystal orientation of the sample [15]. X-ray diffraction and XRF will analyze the powder filtrate in the precipitation to analyze the type of compound of the powder.

Scanning electron microscope (SEM) is an instrument that determines the morphology or crystal structure on the surface of a solid sample through an image. Energy dispersive X-ray (EDX) is an instrument to analyze the chemical elements or characteristics of a material. The residue from the deposition will also be characterized using SEM and EDX to determine the morphology and chemical characteristics of the sample.

5. Result of the research on electrolysis of ferronickel followed by controlled precipitation at moderately acidic pH and elevated temperature

5. 1. Observation of electrolysis time on Ni and Fe dissolved in electrolyte

Fig. 2 shows the relationship between electrolysis time (in hours) and the composition of nickel (Ni) and iron (Fe) in electrolyte(g/L). The nickel contained after 1 hour electrolysis is approximately 5.36 g/l, then rises reaching about 32.57 g/l by the 8th hour. This increase indicates a linear relationship between electrolysis time and Ni composition, with a consistent increase throughout the duration, and it is a common phenomenon in electrochemical reactions [16].

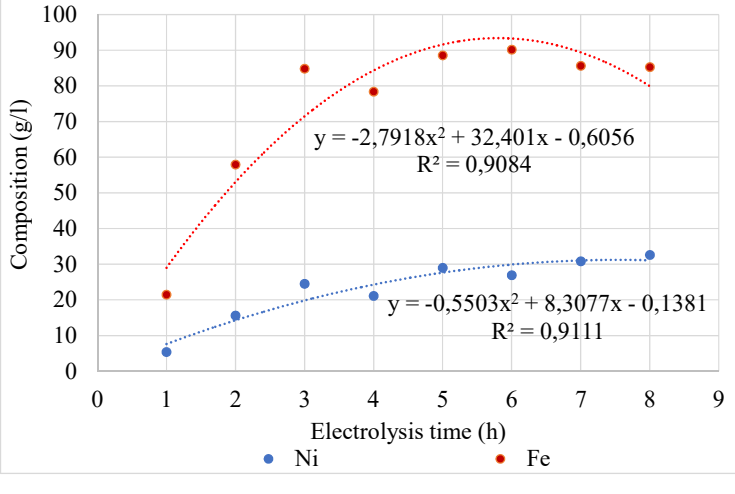

Fig. 2. Dissolved Ni and Fe resulting from electrolysis at 2 M HCl, 2 V were measured using atomic absorption spectrometers based on differences in electrolysis time

The Fe composition increases significantly from around 21.45 g/l at 1 hour to approximately 84.80 g/l by the 3rd hour. After this rapid increase, the composition stabilizes, fluctuating slightly between 78 and 85 g/l from the 4th to the 8th hour. Based on that data, Fe shows a more complex pattern; that is, the Fe composition increases rapidly at the beginning, and it reaches the highest point after a certain period. However, the iron composition stabilizes after this rapid increase, fluctuating between 78 and 85 g/l from the 4th to the 8th hour, suggesting a saturation point. The highest concentration after 6 hours of electrolysis is 90.13 g/l.

5. 2. Phase analysis during the precipitation process with different temperature and pH variation

After the electrolysis with HCl, the electrolyte is rich in Fe, Ni, and other elements. The Precipitation process begins with oxidations using H_2O_2 and continues to precipitate in PH 4.4 and 4.7. Fig. 3 illustrated XRD patterns of precipitates synthesized with a fixed pH of 4.4 and different reaction temperatures of 40°C, 50°C, 60°C, and 70°C. At 40°C, the peaks of a mixed-phase composition of FeO_2 and NiO are shown. The intensity of FeO_2 peaks increases upon the rise in temperature to 50°C, indicating an enhancement in the crystallinity of the phase. The sharpness of the peaks, particularly for NiO, increases at 60°C, indicating a more excellent crystallinity of these phases. At 70°C, FeO_2 and NiO phases are shown to have highest intensities.

According to the analysis of XRD pattern of Fig. 4, the influence of temperature on the formation of phases in precipitation at pH 4.7 exhibits a definite trend in the crystallization of iron oxide and nickel oxide. At 40°C, XRD peaks are broad and of low intensity, which reveals the existence of low crystallized phases. FeO_2 and NiO diffraction peaks are in low intensity, meaning the formed phases are in low quantity. At 50°C, the peaks of FeO_2 and NiO become more defined. The NiO peak become higher than at 40°C, it corresponding to the increasing quantity of NiO. The formation peak of Fe_3O_4 is first observed at very low intensity, showing that the crystalline phase is still developing but is still transitional. The development occurs at 60°C, where the typical diffraction peaks show the occurrence of Fe_3O_4 (magnetite), showing that temperature increase facilitates the structural reorganization of iron oxides to make the formation of stable crystalline phases possible.

Based on Fig. 4 at 70°C, the XRD pattern becomes sharper and higher for NiO peak intensity. The NiO peak at this temperature has the highest intensity, meaning that nickel oxidation is more favorable. The peak of Fe_3O_4 is dimmish, but the peak of FeO_2 peak becomes sharper and well-defined, meaning a higher crystallinity and indicating the oxidation reaction to be more facilitated at higher temperatures. The increased temperature favors the process of crystallization in which Fe_3O_4 forms at 60°C and, at 70°C, is transformed into FeO_2 and NiO, indicating that elevated temperature strengthens phase transformation and are favorable for the oxidation of iron and nickel to yield well-crystallized oxide phases.

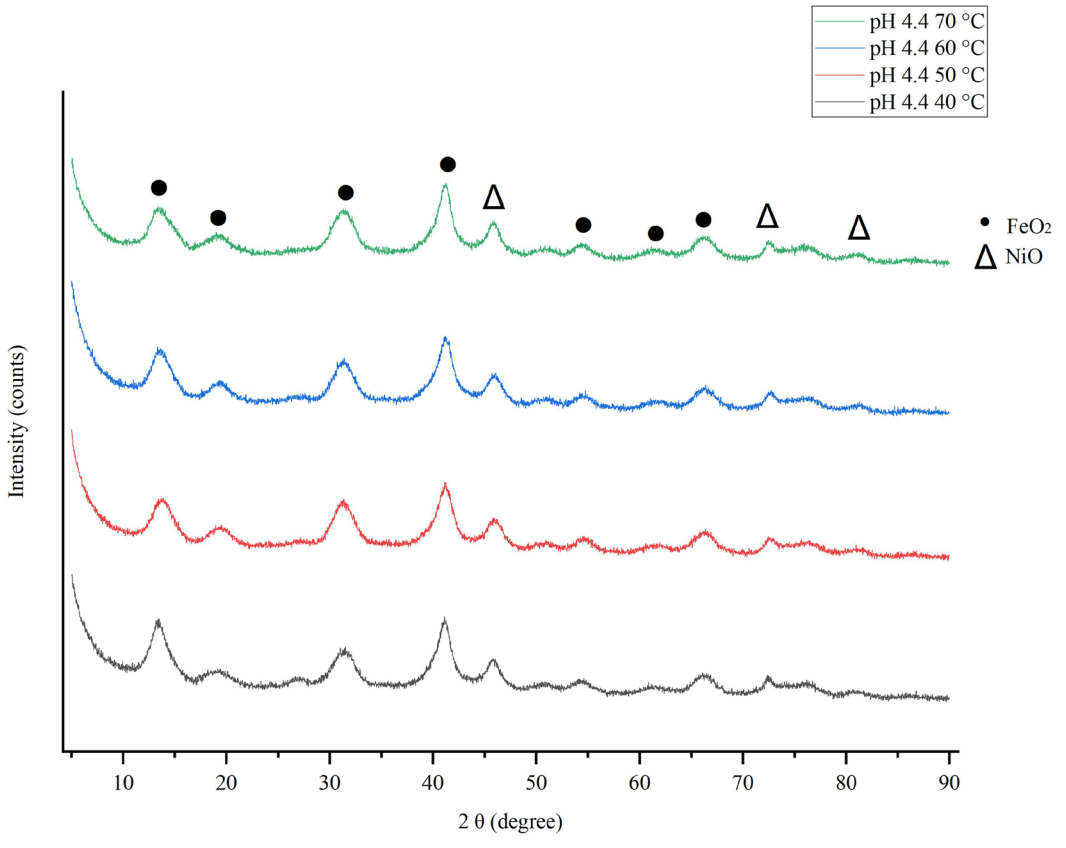

Fig. 3. X-ray diffraction patterns depict the precipitates formed at a constant pH of 4.4 with varying reaction temperatures of 40°C, 50°C, 60°C, and 70°C resulting from electrolysis at 2 M HCl, 2 V for were measured using X-ray diffraction

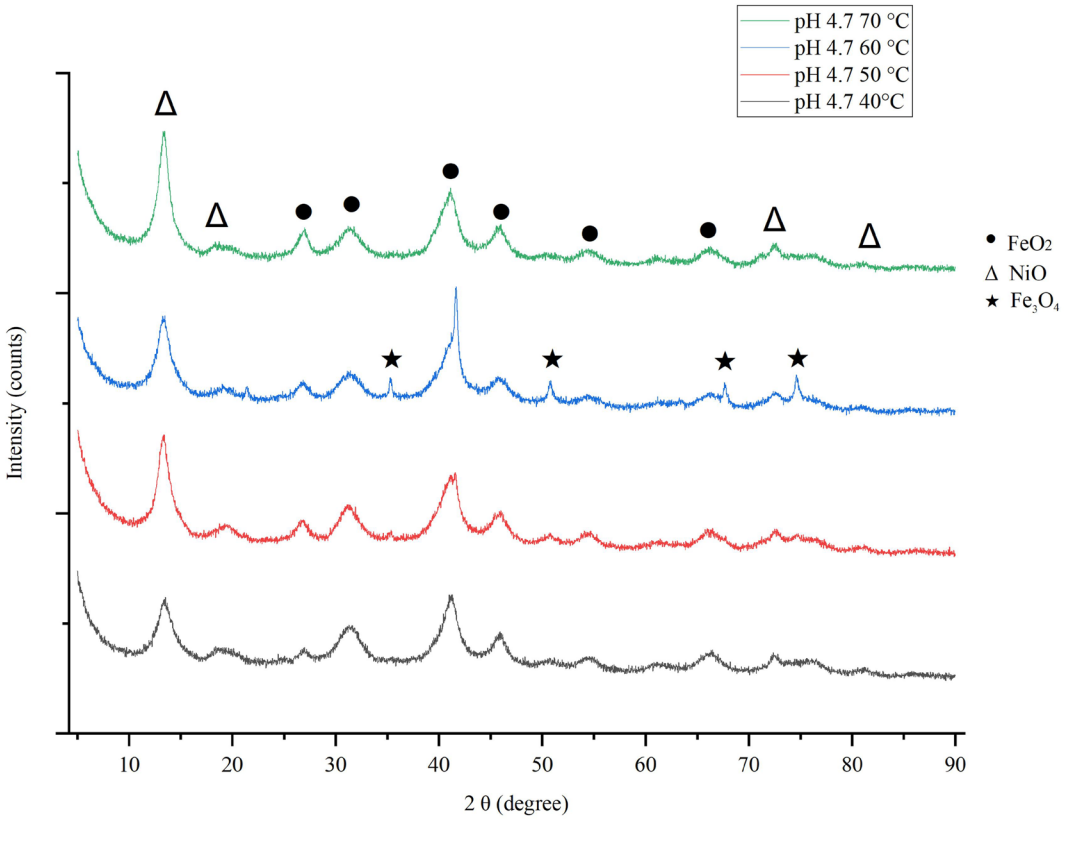

Fig. 4. X-ray diffraction patterns depict the precipitates formed at a constant pH of 4.7 with varying reaction temperatures of 40 ℃, 50°C, 60°C, and 70°C resulting from electrolysis at 2 M HCl, 2 V were measured using X-ray diffraction

5. 3. Composition of the precipitated by XRF analysis

At pH 4.4, the concentrations of Ni (nickel) and Fe (iron), in precipitation had various trends with the rising temperature from 40°C to 70°C (Fig. 5, *a*). The Ni concentration in precipitation rises slightly with the rising temperature, even though its value is always the lowest among the other two elements, manifested in the fact that at 40°C, the Ni content is the lowest compared to other precipitation temperatures. The concentration of Fe in precipitation is very high at all temperature variations and even increases or remains high with the increase in temperature. The highest Fe contains is at 70°C which is 78.91%. This phenomenon indicates that Fe precipitates more efficiently with higher temperatures.

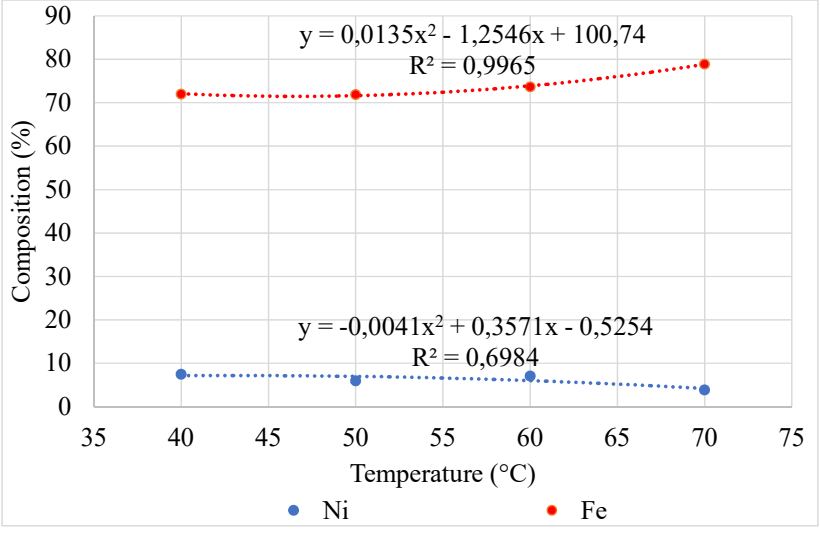

a

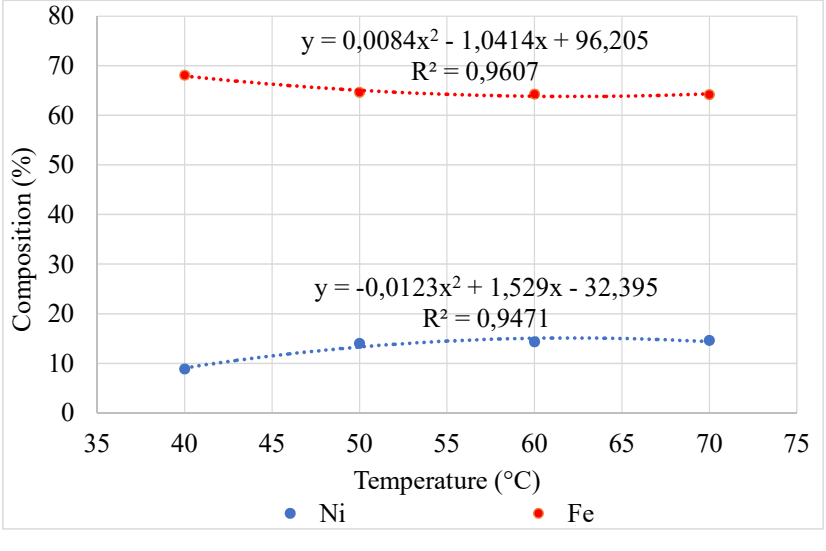

b

Fig. 5. X-ray fluorescence composition analysis depict the precipitates formed with varying reaction temperatures of 40 °C, 50 °C, 60 °C, and 70 °C resulting from electrolysis at 2 M HCl, 2 V at a constant pH: *a* — pH 4.4; *b* — pH 4.7

The differences in the composition of Ni and Fe in precipitation (which comes as a result of their precipitation at pH 4.7) provide proof of the changes in stability of the oxide compounds of these metals corresponding to pH (Fig. 5, *b*). Amounts of iron that were previously highest at pH 4.4 have now declined to within the range of 64% to 68%. While the increasing amounts of precipitation of Nickel are estimated at approximately 14% which supports the fact that 4.7 is closer to the value of pH for the precipitation of $Ni(OH)_2$ (pH 5.5–6). This indicates that greater amounts of Ni are precipitated with increases in pH, even when concentrations of Ni are low. The value of maximum Ni content at 70°C is recorded at 14.60%.

5. 4. Morphology and composition of the precipitated by SEM & EDAX analysis

The SEM analysis compares the surface morphology of precipitates formed at pH 4.4 and 40°C with those formed at pH 4.4 and 70°C (Fig. 5). The first SEM image (*a*), corresponding to pH 4.4 and 40°C, shows a relatively coarse structure with larger and irregularly shaped particles. The particles are loosely packed with a particle size of 6.496 μm, indicating incomplete precipitation under this condition. The second SEM image (*b*) for precipitation at pH 4.4 and 70°C shows a finer with the particle is 916.76 nm, more homogeneous structure with smaller particles. This suggests greater precipitation efficiency at high temperature and pH, and thus improved particle formation and agglomeration.

Table 2

Energy dispersive X-ray spectroscopy analysis result

Element	Weight%			
	Region 1	Region 2	Region 3	Point 1
C	8.3	5.9	6.4	8.7
O	33.5	30.6	30.6	28.2
Cr	1.8	0.0	0.0	0.0
Fe	47.1	50.9	55.6	49.1
Ni	9.3	12.6	7.4	14.0

EDAX analysis measures the composition in a small area, not representing the whole composition. The main phase of the precipitation at pH 4.4 (Table 2) in the region 1 (Fig. 7) is an iron oxide containing around 47.1% Fe and 9.3% Ni. The region 2 composition is an iron oxide containing around 50.9% Fe and 12.6% Ni. Elements with higher atomic numbers reflect more backscattered electrons, resulting in areas rich in heavy elements producing stronger BSE signals and appearing brighter in BSE images [17]. Conversely, regions composed of lighter elements (lower Z) reflect fewer electrons and thus appear relatively darker. This type of contrast is commonly referred to as compositional contrast and is particularly useful for revealing the distribution of heavy elements within heterogeneous samples.

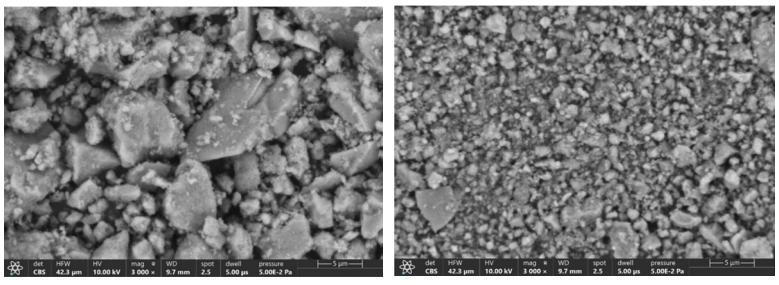

a *b*

Fig. 6. Scanning electron microscope image of:
a — precipitates formed at pH 4.4 and temperatures 40°C;
b — precipitates formed at pH 4.4 and temperatures 70°C

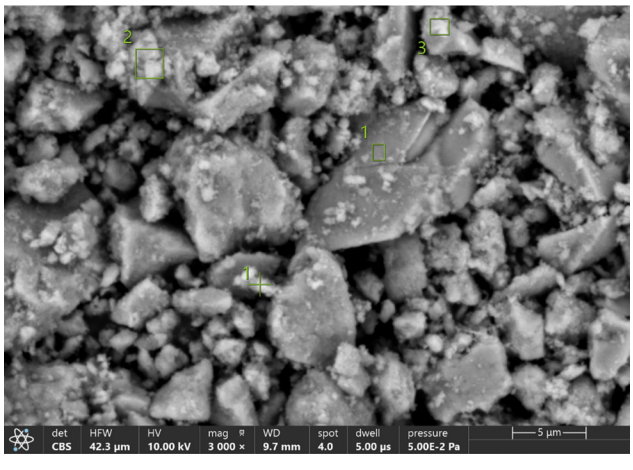

Fig. 7. Energy dispersive X-ray spectroscopy analysis of precipitates formed at pH 4.4 and temperatures 40 ℃

6. Discussion of the time effect in electrolytic dissolution and effect pH and temperature in precipitation for selective nickel purification from ferronickel

This study demonstrates that electrolysis effectively dissolves Ni, Fe, and other elements at room temperature. Unlike the leaching process, which typically requires pretreatment, pressured, and elevated temperatures [7, 8], electrolysis can proceed directly without any pretreatment. During the electrolysis with ferronickel anodes and graphite cathodes, the Fe composition increases significantly from around 21.45 g/l at 1 hour to approximately 84.80 g/l by the 3rd hour (Fig. 2). After this rapid increase, the composition stabilizes, fluctuating slightly between 78 and 85 g/l from the 4th to the 8th hour. In ferronickel anodes, the elements (iron, nickel, etc.) can be oxidized releasing ions into the solution. Iron has the easiest (most negative) oxidation potential among these three metals. The standard reduction potential of Fe^{2+}/Fe is approximately −0.44 V, which is more negative than Ni^{2+}/Ni which is approximately −0.25 V [18]. This means that thermodynamically iron is more easily oxidized (releasing electrons) than nickel. This id due to the passivation phenomenon of Fe metals in acidic environments has been extensively studied. The electrochemical oxide film model further explains the passivation stage, wherein the concentration of anodic metal ions initially rises rapidly and then slows down following the formation of a passive film. All these findings are consistent with the experimental data, which show a high initial metal dissolution rate that decreases during the subsequent phase [19].

Nickel is nobler than iron, so nickel tends to dissolve more slowly unless the anode potential is high enough to oxidize it. After 1 hour of electrolysis, the nickel content is approximately 5.36 g/l, then rises to about 24,46 g/l by the 3rd hour and 32.57 g/l by the 8th hour. This shows an increase which means that the electrolysis time and Ni composition have a linear relationship that increases in value over time, and this relates to a common observation in electrochemical reactions. Temperature and time are important conditions for any reaction, as temperature excites more molecules to become activated and time ensures that the reaction proceeds adequately. However, after 3 hours of electrolysis, the increase is insignificant compared to 1 hour to 3 hours due to the passivation process that needs more investigation.

Unlike previous studies [8, 9] that avoided using raw ferronickel anodes due to their low Ni content, this study demonstrates that direct use of ferronickel is feasible when electrolysis parameters such as time, voltage, and HCl concentration [12] are optimized. This simplifies the process and reduces the need for pretreatment.

The precipitation process begins with oxidations using H_2O_2 and continues to precipitate in PH 4.4 and 4.7 using NaOH with temperature variation. This pH is an early step of the precipitation process to remove Fe, Cr, and other element that precipitate at lower pH. Based on the XRD analysis of the precipitate at pH 4.4 (Fig. 3), the sharpness of the NiO peak increases at 60°C, indicating a more excellent crystallinity of these phases. At 70°C, FeO_2 phases have the highest intensities. This is in line with the results of XRF, which showed an increase in Fe content with increasing temperatures, which experienced a significant increase in precipitation, so the Ni level in precipitation decreased. It explains that as temperature excites, more molecules become activated [20]. Increasing temperature resulted increasing Fe removal in synthetic laterite leach solution [7]. Based on the Pourbaix diagram [21], the pH for Fe precipitation is lower than Ni precipitation. So, it gives a chance for Fe to precipitate. Furthermore, at pH 4.4 is favorable for Fe removal because this pH minimizes the Ni loss.

The XRD pattern becomes sharper and higher for NiO peak intensity at pH 4.7 at 70°C (Fig. 4). The NiO peak at this temperature has the highest intensity, meaning that nickel oxidation is more favorable. The increased temperature favors the process of crystallization in which Fe_3O_4 forms at 60°C and, at 70°C, is transformed into FeO_2 and NiO, indicating that elevated temperature strengthens phase transformation and are favorable for the oxidation of iron and nickel to yield well-crystallized oxide phases. The phase transition is possible due to increasing the temperature [21]. This is further supported by XRF results (Fig. 5) showing that with increased temperatures, there is an increase in Ni proportion. The highest recorded value for Ni component content is at 70°C and 14.60%. When comparing Ni level at 70°C and pH 4.4, which is 3.89%, it can be observed that pH 4.7 is not ideal to deplete Fe content from the solution because it can lead to greater loss of Ni. At a pH of 2 to 8, depending on the energy, Fe^{2+} can precipitate. Fe^{3+} can precipitate at pH 2, however, it is suggested that Fe^{3+} is optimally precipitated

first. Analyzing the Pourbaix diagram [22], Fe precipitated at a lower pH than Ni. Ni is expected to precipitate at a high pH of 9 but did begin to precipitate at pH values of 7 to 8.

The morphology and particle size of precipitate at pH 4.4 was examined by SEM. Fig. 6, *a* shows SEM image of precipitate at 40°C, revealing a relatively coarse structure with larger and irregularly shaped particles. The particles are loosely packed with a particle size of 6.496 μm, indicating incomplete precipitation under this condition. Fig. 6, *b* shows SEM image of precipitate at 70°C, shows a finer with the particle is 916.76 nm, more homogeneous structure with smaller particles. This suggests greater precipitation efficiency at high temperature and pH, and thus improved particle formation and agglomeration. Optimal conditions lead to smaller nanoparticle sizes under specific interactions, correlating with the observed phenomenon that increased temperature can favor smaller precipitate particles [23]. Fig. 7 shows the EDAX analysis and also the result of the analysis. It revealed that the brighter area contains lower nickel than darker area [18].

The electrolysis and precipitation approach is currently demonstrated under controlled laboratory conditions using specific concentrations (2 M HCl), fixed voltages (2 V), and selected temperature and pH ranges. Therefore, the applicability of the results may be limited when scaled up to industrial operations, which often involve more complex systems, fluctuating feed compositions, and different environmental constraints. The reproducibility of the results depends on the consistency of the ferronickel composition, electrolyte purity, and precise control of electrochemical parameters.

The disadvantage of this study is the effectiveness of separation may be sensitive to slight variations in pH and temperature. The current findings are adequate within the tested range of electrolysis time (1–8 hours) and temperature (40–70°C), and further validation is needed to confirm their stability under extended operational durations or higher throughput conditions. In this study, higher pH levels such as 4.7, increase nickel precipitation but compromise iron removal efficiency. In future research, precipitation can be done step by step, first using pH 4.4 to precipitate Fe with minimalizing Ni loss, and second precipitation using pH 9 to precipitate Ni.

7. Conclusions

1. Electrolysis time strongly influences Ni vs. Fe dissolution. Extending electrolysis in 2 M HCl (2 V) yielded a nearly linear increase in dissolved Ni: from ≈5.36 g/l at 1 h to 32.57 g/l by 8 h. In contrast, Fe dissolved very rapidly at first (≈84.8 g/l by 3 h) then reached a plateau (fluctuating ~78–85 g/l after 4–8 h, with a maximum of ≈90.1 g/l at 6 h). These results indicate that prolonged electrolysis continuously enhances Ni extraction, whereas Fe concentration saturates after ~3 h, defining an optimal time frame for selective Ni enrichment in the electrolyte.

2. Precipitation pH determines the oxide phases formed. XRD analysis showed that precipitates formed at pH 4.4 consisted predominantly of FeO_2 and NiO, with increasing crystallinity as temperature rise (NiO peak sharpened at 60°C and both FeO_2/NiO peaks were strongest at 70°C). At pH 4.7, low-temperature precipitates were poorly crystalline (broad, weak peaks), but heating to 60°C first produced magnetite (Fe_3O_4) which then transformed to FeO_2 by 70°C. Simultaneously, the NiO peak became highest at 70°C (indicating favorable nickel oxide formation). Thus, raising pH from 4.4 to 4.7 shifts the phase evolution: an intermediate Fe_3O_4 phase appears at ~60°C and a well-crystallized NiO phase dominates at higher temperature, whereas at pH 4.4 only FeO_2/NiO phases were observed.

3. Precipitate composition depends on pH and temperature. XRF results demonstrated that at pH 4.4 the solids were Fe-rich (Fe≈78.9 wt.% at 70°C) with very low Ni content, while at pH 4.7 the Fe fraction decreased (~64–68 wt.%) and Ni incorporation increased (up to 14.6 wt.% Ni at 70°C). Increasing temperature generally promoted precipitation of all metals, with Fe fractions rising at higher T. Notably, the maximum Ni recovery (14.60 wt.%) occurred at pH 4.7 and 70°C, whereas the highest Fe recovery (78.91 wt.%) occurred at pH 4.4 and 70 °C. This indicates that adjusting pH toward 4.7 is not ideal to deplete Fe content from the solution because it can lead to greater loss of Ni.

4. Higher precipitation temperature produces finer precipitate morphology. SEM imaging revealed that at pH 4.4 the precipitate formed at 40°C had a coarse, loosely packed structure with large, irregular particles (average size ≈6.50 μm). By contrast, at 70°C the precipitate was much finer and more homogeneous, with particles ~916.8 nm (≈0.92 μm). The denser, submicron-scale morphology at higher temperature reflects improved crystallization and aggregation, implying more efficient precipitation. In summary, increasing precipitation temperature (with pH held constant) dramatically reduces crystal size and refines particle morphology in the Ni-Fe oxide precipitate.

Conflict of interest

The authors declare that they have no conflict of interest in relation to this study, whether financial, personal, authorship or otherwise, that could affect the study and its results presented in this paper.

Financing

Universitas Indonesia financially supported this work through the PUTI Postgraduate Grant with contract number NKB-246/UN2.RST/HKP.05.00/2023.

Data availability

Data will be made available on reasonable request.

Use of artificial intelligence

The authors confirm that they did not use artificial intelligence technologies when creating the current work.

Acknowledgment

The authors would also like to thank PT ANTAM Tbk. for providing the FeNi material.

References

1. Chung, J. (2025). The Mineral Industry of Indonesia. U.S. Geological Survey. Available at: https://pubs.usgs.gov/myb/vol3/2022/myb3-2022-indonesia.pdf
2. Arif, I. (2018). Nikel Indonesia. Gramedia Pustaka Utama, 276.
3. Handayani, L. (2024). Ditjen ILMATE: 44 Smelter Nikel Beroperasi di Indonesia. Media Nikel Indonesia. Available at: https://nikel.co.id/2024/03/20/ditjen-ilmate-44-smelter-nikel-beroperasi-di-indonesia/
4. Xue, Y., Zhu, D., Pan, J., Guo, Z., Yang, C., Tian, H. et al. (2020). Effective Utilization of Limonitic Nickel Laterite via Pressurized Densification Process and Its Relevant Mechanism. Minerals, 10 (9), 750. https://doi.org/10.3390/min10090750
5. Moussoulos, L. (1975). A process for the production of electrolytic nickel from ferronickel. Metallurgical Transactions B, 6 (4), 641–645. https://doi.org/10.1007/bf02913860
6. Han, H., Sun, W., Hu, Y., Cao, X., Tang, H., Liu, R., Yue, T. (2016). Magnetite precipitation for iron removal from nickel-rich solutions in hydrometallurgy process. Hydrometallurgy, 165, 318–322. https://doi.org/10.1016/j.hydromet.2016.01.006
7. Das, G. K., Li, J. (2023). Iron Removal as Goethite from Synthetic Laterite Leach Solutions. ACS Omega, 8 (13), 11931–11940. https://doi.org/10.1021/acsomega.2c07595
8. Zunaidi, M. A., Setiawan, I., Oediyani, S., Irawan, J., Rhamdani, A. R., Syahid, A. N. (2022). Iron removal process from nickel pregnant leach solution using sodium hydroxide. Metalurgi, 37 (3). https://doi.org/10.14203/metalurgi.v37i3.665
9. Viswanath, S. G., Jachak, M. M. (2013). Electrodeposition of nickel powder from nickel sulphate solution in presence of glycerol and sulphuric acid. Metall. Mater. Eng., 19 (3), 233–248.
10. Shih, Y.-J., Chien, S.-K., Jhang, S.-R., Lin, Y.-C. (2019). Chemical leaching, precipitation and solvent extraction for sequential separation of valuable metals in cathode material of spent lithium ion batteries. Journal of the Taiwan Institute of Chemical Engineers, 100, 151–159. https://doi.org/10.1016/j.jtice.2019.04.017
11. Partinen, J., Halli, P., Wilson, B. P., Lundström, M. (2023). The impact of chlorides on NMC leaching in hydrometallurgical battery recycling. Minerals Engineering, 202, 108244. https://doi.org/10.1016/j.mineng.2023.108244
12. Astini, V., Meirawati, S., Nengsih, S., -, A., -, H., Soedarsono, J. W. M., Zulfia, A. (2024). Influence of Electrolyte Molarity and Applied Voltage on the Purification of Ferronickel by Electrolysis Method. Metalurgi, 39 (1), 7. https://doi.org/10.55981/metalurgi.2024.742
13. Linnikov, O. D., Rodina, I. V., Zakharova, G. S., Mikhalev, K. N., Baklanova, I. V., Kuznetsova, Y. V. et al. (2022). Coagulation removal of nickel (II) ions by ferric chloride: Efficiency and mechanism. Water Environment Research, 94 (12). https://doi.org/10.1002/wer.10827
14. Sanz-Medel, A., Pereiro, R. (2014). Atomic absorption spectrometry: An introduction. Momentum Press, 205.
15. Luger, P. (2014). Modern X-Ray Analysis on Single Crystals. De Gruyter. https://doi.org/10.1515/9783110308280
16. Speck, F. D., Dettelbach, K. E., Sherbo, R. S., Salvatore, D. A., Huang, A., Berlinguette, C. P. (2017). On the Electrolytic Stability of Iron-Nickel Oxides. Chem, 2 (4), 590–597. https://doi.org/10.1016/j.chempr.2017.03.006
17. Ali, A., Zhang, N., Santos, R. M. (2023). Mineral Characterization Using Scanning Electron Microscopy (SEM): A Review of the Fundamentals, Advancements, and Research Directions. Applied Sciences, 13 (23), 12600. https://doi.org/10.3390/app132312600
18. P1: Standard Reduction Potentials by Element. LibreTexts. Available at: https://chem.libretexts.org/Ancillary_Materials/Reference/Reference_Tables/Electrochemistry_Tables/P1%3A_Standard_Reduction_Potentials_by_Element
19. Bösing, I. (2023). Modeling electrochemical oxide film growth—passive and transpassive behavior of iron electrodes in halide-free solution. Npj Materials Degradation, 7 (1). https://doi.org/10.1038/s41529-023-00369-y
20. Shu, R., Zhang, Q., Ma, L., Xu, Y., Chen, P., Wang, C., Wang, T. (2016). Insight into the solvent, temperature and time effects on the hydrogenolysis of hydrolyzed lignin. Bioresource Technology, 221, 568–575. https://doi.org/10.1016/j.biortech.2016.09.043
21. Pangaribuan, R. H., Patrick, J., Prasetyo, A. B., Maksum, A., Munir, B., Soedarsono, J. W. (2018). The effect of NaOH (natrium hydroxide) to slag nickel pyrometallurgy in different temperature and additive ratio. E3S Web of Conferences, 67, 03052. https://doi.org/10.1051/e3sconf/20186703052
22. Takeno, N. (2005). Atlas of Eh-pH diagrams. Intercomparison of thermodynamic databases. Geological Survey of Japan Open File Report No. 419. National Institute of Advanced Industrial Science and Technology. Available at: https://www.nrc.gov/docs/ML1808/ML18089A638.pdf
23. Vajglová, Z., Gauli, B., Mäki-Arvela, P., Kumar, N., Eränen, K., Wärnå, J. et al. (2023). Interactions between Iron and Nickel in Fe–Ni Nanoparticles on Y Zeolite for Co-Processing of Fossil Feedstock with Lignin-Derived Isoeugenol. ACS Applied Nano Materials, 6 (12), 10064–10077. https://doi.org/10.1021/acsanm.3c00620